Validity of Yubero-Tougaard theory to quantitatively determine the dielectric properties of surface nanofilms

Shaaker Hajati,[1,2] Oleksandr Romanyuk,[3] Josef Zemek,[3] and Sven Tougaard[1]
[1]*Department of Physics and Chemistry, University of Southern Denmark, DK-5230 Odense M, Denmark*
[2]*Department of Physics, Yasouj University, Yasouj 75919-353, Iran*
[3]*Institute of Physics, Academy of Sciences of the Czech Republic, Cukrovarnicka 10, 162 53 Prague 6, Czech Republic*
(Received 16 May 2007; revised manuscript received 28 February 2008; published 2 April 2008)

Reflection electron energy-loss spectroscopy (REELS) at low energies is very surface sensitive and can be used to characterize the electronic properties of ultrathin films and surface nanostructures. To extract reliable quantitative information from a REELS experiment it is essential to have accurate theoretical algorithms. In this paper, we have studied the validity of a theoretical method proposed by Yubero and Tougaard [Phys. Rev. B **46**, 2486 (1992); Phys. Rev B **53**, 9719 (1996)] to determine the dielectric function ε by using an analysis of an effective experimental REELS cross section determined by the Tougaard–Chorkendorff algorithm [Phys Rev B **35**, 6570 (1987)]. To this end, REELS experiments with electrons incident normal to the surface were carried out for a wide range of exit angles (35°–74° to the surface normal) and energies 200, 500, and 1000 eV for several materials (Cu, Ag, Au, and Fe). We find that the theory is in very good agreement with experiment for all geometries and energies studied. It is important to note that for a given element, the same ε is used for all geometries and energies and that this ε is determined by the analysis. The fact that the theory applies at energies at least down to 200 eV where the inelastic mean free path (λ) is ~0.5 nm implies that the method can be used to determine the dielectric properties of nanofilms, and the additional fact that the theory can predict the variation with angle suggests that the method might also be used to determine the dielectric properties of nanostructures.

DOI: 10.1103/PhysRevB.77.155403 PACS number(s): 79.20.Uv, 73.20.Mf

I. INTRODUCTION

New methods to characterize the electronic properties of surface nanostructures are of great technological importance. Reflection electron energy loss spectroscopy (REELS) at low energy is surface sensitive and capable of detecting the electronic structure (represented by, e.g., the dielectric function $\varepsilon[k, \omega]$) of ultrathin films because when the energetic electron travels in the surface region of a solid, the incident electron can be inelastically scattered through an interaction with valence and core electrons.[1]

Several models have been developed to describe the electron energy loss in a REELS experiment.[2–13] Two approaches have been followed to describe the influence of surface excitation. In 1992, Yubero and Tougaard tested a simple model[6] where surface and bulk excitations were treated as separate events and represented by surface and volume loss functions with a shape that was assumed to be independent of energy and experimental geometry. They found that although they could get a good account of the observed variations in energy loss with primary energy and geometry, the determined expansion coefficients turned out to be unphysical.[6] This led them to conclude that the surface and bulk excitations cannot be treated as separate events. Subsequently, they developed models where the electron trajectory from the electron gun to the electron energy analyzer was treated as a single event.[7,8] They showed that not only the relative intensities but also the shape of surface and bulk energy-loss distribution depend on the energy, geometry, and the depth where the electron is backscattered. Even as the electron travels in the vacuum outside the solid, it will experience significant energy-loss processes. In spite of these findings, other groups have later followed the idea of separating the surface and bulk excitations into two functions, a surface and a bulk term.[5,10–14] For instance, in the model of Chen and co-workers,[5,13,14] the surface loss component is calculated by integrating the surface loss function over all depths, assuming that every electron in the REELS experiment penetrates the full region in which surface losses occur. In other words, it is assumed that all detected electrons experience the same surface effect independent of the depth they reach. Recently, Werner has presented a procedure to decompose experimental loss spectra of medium-energy electrons reflected from solid surfaces into contributions due to surface and volume electronic excitations.[10,11] This was achieved by an analysis of two spectra acquired at two different energies[10] and/or geometrical configurations.[11] The basic assumption in this procedure is thus also that the surface and bulk excitations can be treated as separate events. Although he found a reasonable agreement with experiment, his comparison was limited to only one pair of measurements, which does not necessarily test the validity of the theory. Thus, a thorough test of the validity would require that a series of experiments obtained with a wide range of energies and geometries all give good agreement with theory. Recently, an example was published for Au where two sets of REELS spectra taken at different energies were shown to give similar results.[12] However, both sets were taken at relatively high energies ($\geqslant$1000 eV) where the influence of the surface is less critical.

To be able to use REELS to study the dielectric properties of nanostructures, a low primary electron energy for which the electron inelastic mean free path (λ) is less than the nanostructure dimension, i.e., $\lambda < 1$ nm, is required. There-

 ©2008 The American Physical Society

TABLE I. Determined parameters in the ELF to give the best overall fit to all experimental cross sections for each material.

	i	$\hbar\omega_{0i}$ (eV)	A_i (eV^2)	γ_i (eV)
Ag	1	3.9	0.55	0.37
(E_g=0)	2	8.6	25.18	4.6
(α_i=1)	3	12	6.32	7
	4	17.5	53.17	7.5
	5	24	63.49	5
	6	32.5	35.10	5
	7	47	340.12	30
	8	55	80.24	9
	9	69.5	55.17	8
Au	1	2.9	0.16	0.8
(E_g=0)	2	6.2	3.81	4
(α_i=1)	3	10.15	17.73	6.75
	4	16.6	56.60	8.5
	5	24	130.99	7.5
	6	31.8	113.40	8.5
	7	44.85	231.68	23
	8	61.75	187.23	19
Cu	1	4.3	0.14	0.8
(E_g=0)	2	7.1	0.29	1
(α_i=1)	3	9.95	38.17	7
	4	15	20.69	7.5
	5	18.8	86.07	7.5
	6	26.5	51.87	5
	7	37.5	131.28	45
	8	60.1	176.68	55
	9	79.41	312.46	45
Fe	1	9.4	17	8
(E_g=0)	2	16	70	9
(α_i=1 for $i\leqslant 4$)	3	22	210	10
(α_i=0 for $i\geqslant 5$)	4	30	39	20
	5	57	47	7
	6	68	63	18

fore, theory must be applicable to describe the REELS experiments at $E<500$ eV, where λ is typically less than 1 nm.[15]

In the present work, we have made an extensive test of the validity of the dielectric response REELS model proposed by Yubero and Tougaard.[7,8] This theory was implemented in the QUEELS-$\varepsilon(k,\omega)$-REELS software,[9] which we used to carry out a quantitative analysis of the REELS spectra. In the following, we will refer to this as the YT model. The model takes into account bulk and surface contributions and the interference effects of the electric field setup by the incident electron on the reflected electron. It also includes the energy loss that occurs while the electron travels in the vacuum due to its interaction with its image charge. This model was previously found to give a good quantitative agreement with

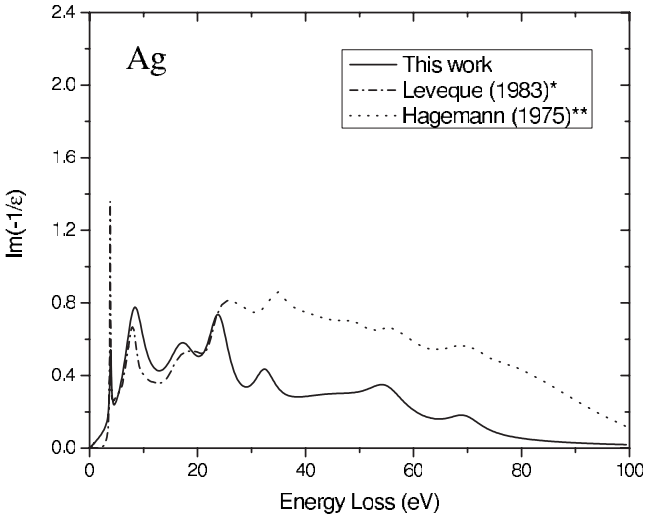

FIG. 1. The determined ELF of Ag compared to the optical data. * Reference 34 taken from Palik (Ref. 31). ** Reference 33 taken from Palik (Ref. 31).

experiment.[8,16,17] It provides a straightforward way to determine the energy-loss function and thereby the electronic properties of a solid and to determine the inelastic-scattering properties. Recently, it was applied to determine electronic properties of ultrathin HfO_2, Al_2O_3, and Hf-Al-O dielectric films on Si (100).[18,19]

As mentioned above, the shape of energy-loss distribution depends on the geometry as well as the depth where the electron is backscattered, and this is taken into account in the YT model.[7,8] However, there are some assumptions in this theory, and the question is to what extent they limit the validity of the YT model. The two main assumptions are the procedure to determine an effective experimental single scattering cross section and the simple model used to describe elastic electron scattering.

The first possible problem originates from the procedure used to deduce the experimental cross section from the measured REELS spectrum. This is done with the method of Tougaard and Chorkendorff,[20] which relies on a theory where the path-length distribution is assumed to be a simple exponentially increasing or decreasing distribution over the relevant range of path length (i.e., $\leqslant 3\lambda$). The method corrects for multiple scattered electrons and gives an effective single scattering cross section. This cross section is, however, not strictly the single scattering cross section. The reason, as explained in the paper by Tougaard and Chorkendorff,[20] is that their algorithm relies on the assumption that as the electron travels in the solid, the probability for energy loss ΔE is a constant function of ΔE independent of the actual depth underneath the sample surface. It is, however, clear that the probability of exciting a surface plasmon decreases and the probability of exciting a bulk plasmon increases with depth. Therefore, the relative intensities in the various multiple surface and bulk plasmon peaks will be slightly different.[20,21] This effect is mainly seen for materials such as Al and Si with narrow surface and bulk plasmon peaks at distinctly different energy losses. This issue was also addressed recently by Werner.[10,11] However, even for Al

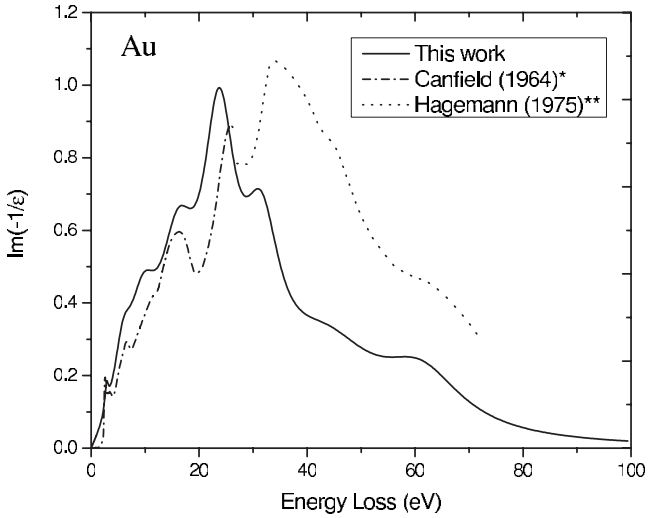

FIG. 2. The determined ELF of Au compared to the optical data. * Reference 35 taken from Palik (Ref. 31). ** Reference 33 taken from Palik (Ref. 31).

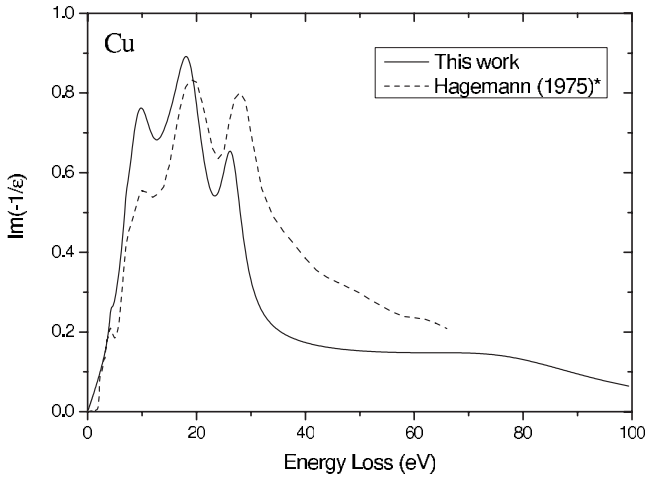

FIG. 3. The determined ELF of Cu compared to the optical data *. Reference 33 taken from Palik (Ref. 31).

and Si the agreement between theory and experiment is good for energy loss less than the sum of surface and bulk plasmon energies.[7,17,22] Most materials have wider energy-loss structures, and the effect is expected to be small. However, we want to test how important this possible problem is. The degree of mixing surface and bulk excitations in the theoretical single scattering cross section K_{th} will depend on the energy and geometry. Thus, at 200 eV and a 74° exit angle to the surface normal, the mixture will be very different from the situation at 1000 eV and 35° exit angle. We can therefore test the possible influence of this effect on the validity of the *Y-T* model by comparing calculated K_{th} to the experimental effective single scattering cross section for this wide range of energies and angles using the same dielectric function ε in all calculations for a given material.

The second problem may arise because of the simple model used to account for elastic electron scattering in which the YT model assumes the electron trajectories to be V type; i.e., their trajectory inside the solid is determined by a single large angle scattering event. Even with this assumption, the resulting theoretical expression is rather complicated. It would therefore hardly be manageable to consider, within their model, more general trajectories where the electrons have been elastically scattered several times. However, both the incidence and the exit angles are correct for all detected electrons regardless of the elastic-scattering processes inside the solid because they are determined by the position of the electron gun and the electron energy analyzer. Furthermore, detailed Monte Carlo calculations show that most of the observed REELS electrons in the energy range of interest have indeed undergone a single large-angle scattering event.[23] However, these assumptions might not be sufficiently accurate, and we will test the range of the validity here. If, for a given REELS geometry, the probability for elastic scattering into the direction of the detector is large, then the majority of the detected electrons will have undergone a single scattering event. If it is small, the role of multiple scattering will be larger. Therefore, the possible failure of the YT model for elastic scattering will be most critical at angles where the single elastic-scattering cross section is small. We therefore study this issue at all angles in the range 35°–74° to test for a possible problem when a deep minimum in the elastic-scattering cross section occurs for the angle between the electron gun and analyzer.

In this paper, we have thus investigated the limits of applicability of the YT model to determine the dielectric properties of nanofilms. We compare the calculated and experimental cross sections for materials Cu, Ag, and Au at energies 200, 500, and 1000 eV and for Fe at energies 200 and 500 eV for normal incidence and emission angles from 35° to 74° with a 3° angle step. We find that using the YT method, we can determine a dielectric function $\varepsilon\ (k,\omega)$ that consistently describes all experiments quantitatively. Thus, without varying ε, we find that the theory gives a consistently good agreement with experiment at both high and low energies, exit angles close to surface normal, and at very glancing angles.

II. THEORY

A. Inelastic-scattering cross sections from reflection electron energy loss spectroscopy

Let a beam of electrons of energy E_0 be incident on the sample surface and let $j_l(E)$ be the measured energy distribution of REELS electrons. Now, assume that the sample is a homogeneous medium in the sense that as the electron travels in the solids, the probability $K(E_0,T)$ for energy-loss T per unit path length and per unit energy loss is a constant function of T, independent of the actual depth underneath the solid surface. Then, assuming that the distribution of path lengths R can for $R<3\lambda$ be approximated by $e^{-R/L}$, where the decay length L can take either positive or negative values,[20,21] the effective experimental electron inelastic cross section $K_{\mathrm{exp}}(E_0,T)$ is determined from an experimental REELS spectrum as[20,21]

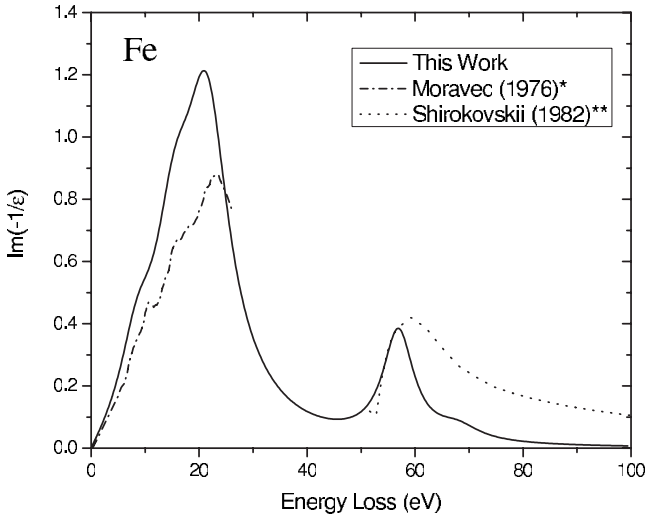

FIG. 4. The determined ELF of Fe compared to the optical data. * Reference 36 taken from Palik (Ref. 32) ** Reference 37 taken from Palik (Ref. 32).

$$\lambda^* K_{\mathrm{exp}}(E_0, E_0 - E) = \frac{j_l(E) - \int_E^{E_0} \lambda^* K_{\mathrm{exp}}(E_0, E' - E) j_l(E') dE'}{\int_{E_0^-}^{E_0^+} j_l(E') dE'}, \quad (1)$$

where the denominator is the area of the elastic peak and

$$\lambda^* = \lambda L/(\lambda + L), \quad (2)$$

where L can be obtained if λ^* and λ are known

$$L = \lambda\lambda^*/(\lambda - \lambda^*). \quad (3)$$

For a numerical treatment, the REELS spectrum is divided into channels E_i of width δE (with $i=0$ at E_0) to get the following from Eq. (1):

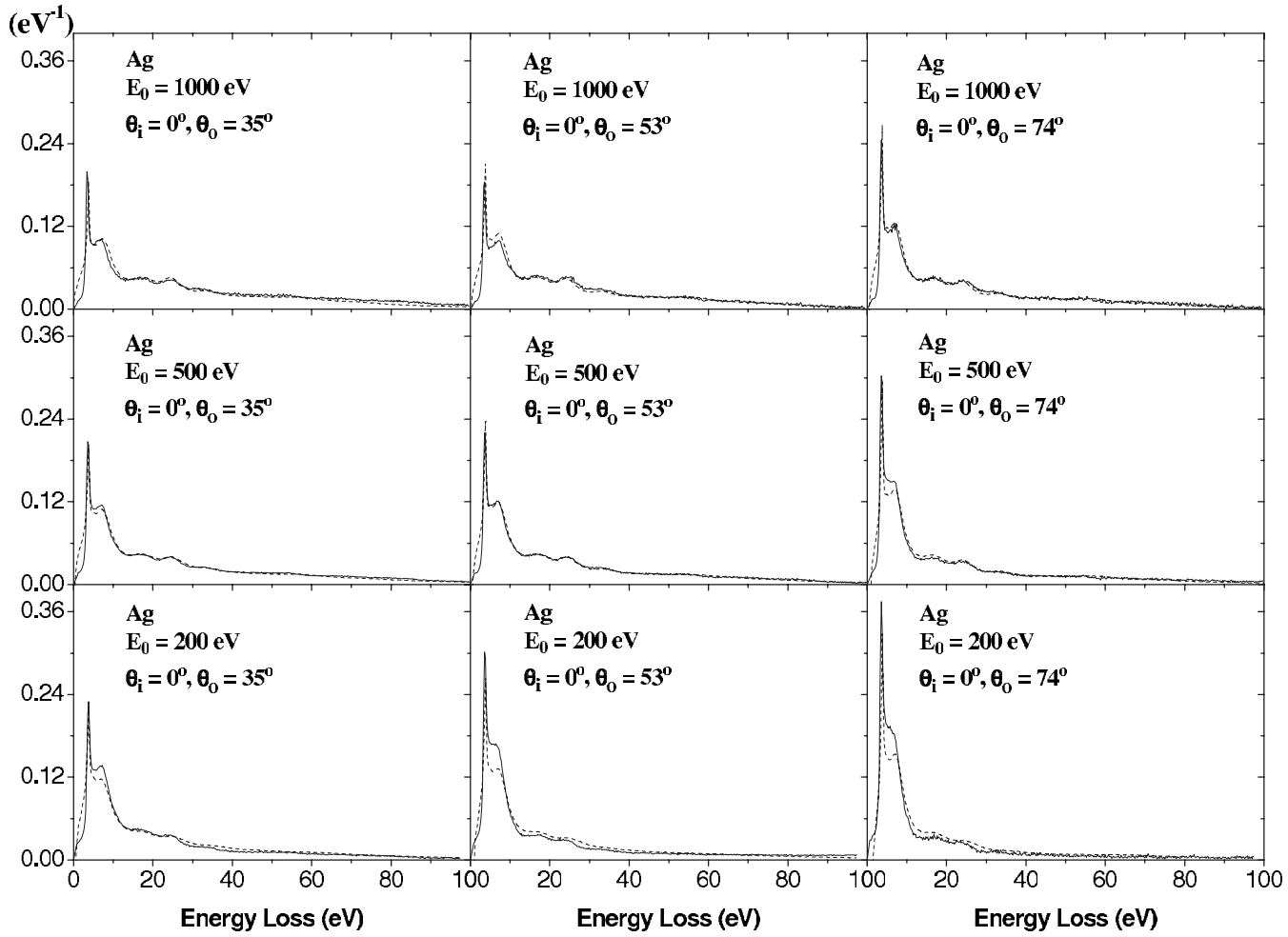

FIG. 5. $\lambda^* K_{\mathrm{exp}}$ (solid line) and $\lambda^* K_{\mathrm{th}}$ (dashed line).

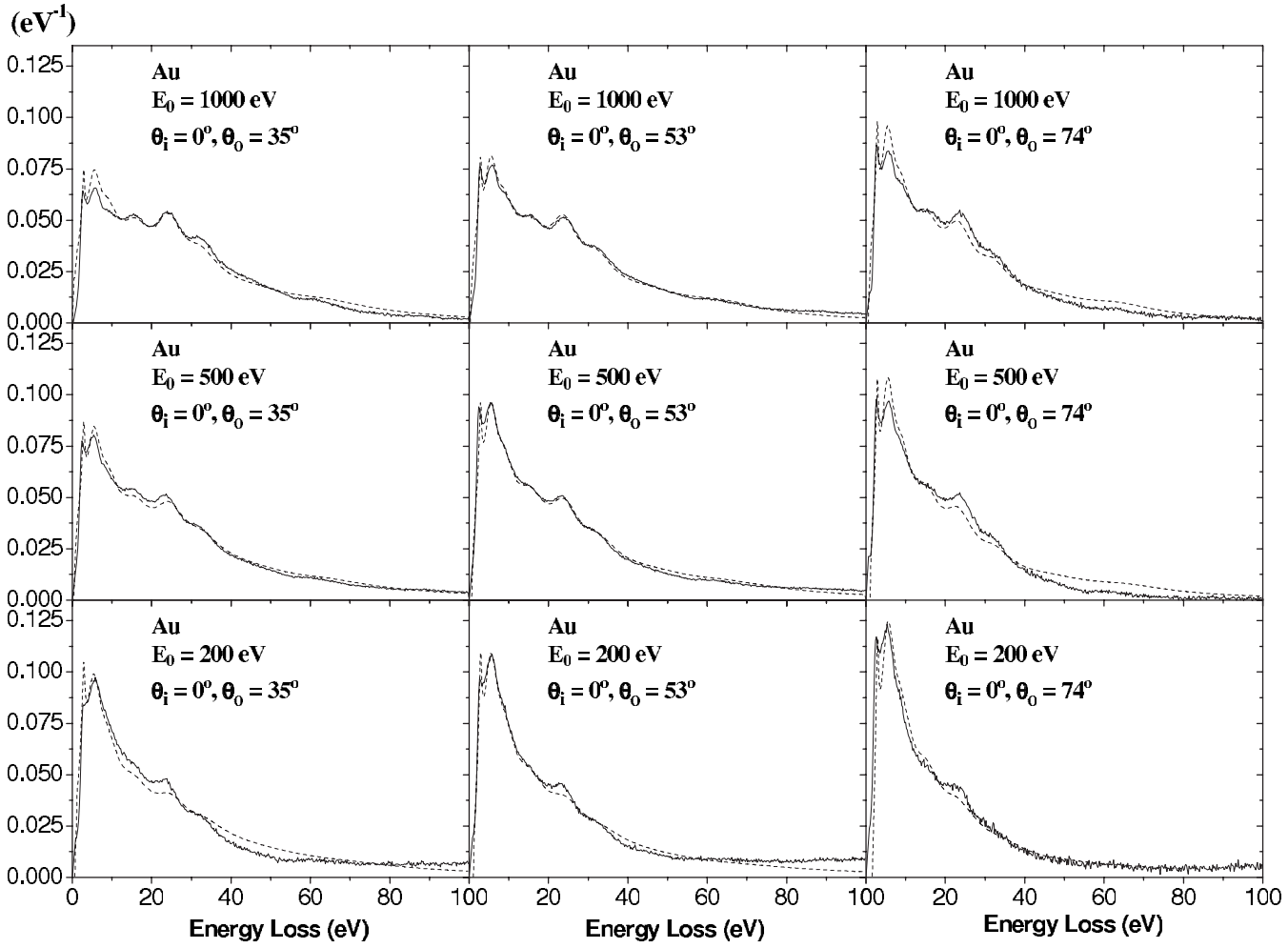

FIG. 6. $\lambda^* K_{\mathrm{exp}}$ (solid line) and $\lambda^* K_{\mathrm{th}}$ (dashed line).

$$\lambda^* K_{\mathrm{exp}}(E_0, E_0 - E_i) = \frac{j_l(E_i) - \sum_{m=1}^{i-1} \lambda^* K_{\mathrm{exp}}(E_0, E_m - E_i) j_l(E_m)\,\delta E}{A_0}, \quad (1')$$

where A_0 is the area of the elastic peak.

B. Determination of energy-loss functions and inelastic-scattering cross sections from model dielectric functions

The basic ideas and an extensive discussion of the procedure to determine the electron energy-loss function (ELF) from experimental REELS according to the method of YT can be found in Refs. 7–9 and 24–26. The theoretical effective single scattering cross section $K_{\mathrm{th}}(E_0, \Delta E)$ for *all* REELS electrons corresponding to a given REELS experiment can be calculated if the ELF is known. Here, E_0 is the primary electron energy and ΔE is the energy lost by an electron in a scattering event. The ELF of the material is parametrized in terms of an expansion in Drude–Lindhard-type oscillators,[7]

$$\mathrm{Im}\left\{-\frac{1}{\varepsilon(k,\Delta E)}\right\} = \sum_{i=1}^{n} \frac{A_i \gamma_i \Delta E}{((\hbar\omega_{0ik})^2 - \Delta E^2)^2 + \gamma_i^2 \Delta E^2} \times \theta(\Delta E - E_g), \quad (4)$$

with

$$\hbar\omega_{0ik} = \hbar\omega_{0i} + \alpha_i \frac{\hbar^2 k^2}{2m}, \quad (5)$$

where the parameters A_i, γ_i, $\hbar\omega_{0i}$, and α_i are the oscillator strength, damping coefficient, excitation energy, and momentum dispersion coefficient of the i_{th} oscillator, respectively, and $\hbar k$ is the momentum transferred from the REELS electron to the solid. The step function $\theta(\Delta E - E_g)$ simulates a band gap E_g in semiconductors and insulators, so that $\theta(\Delta E - E_g) = 0$ if $\Delta E < E_g$ and $\theta(\Delta E - E_g) = 1$ if $\Delta E > E_g$. The dependence of ω_{0ik} on k is generally unknown, but we use Eq. (5) with α_i as an adjustable parameter. The values of the momentum dispersion coefficients α_i are related to the effective electron mass, so that for free electrons $\alpha_i = 1$ and for flat energy bands $\alpha_i = 0$.

In the calculations, the oscillator strengths in the function $\mathrm{Im}\{1/\varepsilon(0, \Delta E)\}$ are adjusted to make sure that it fulfills the

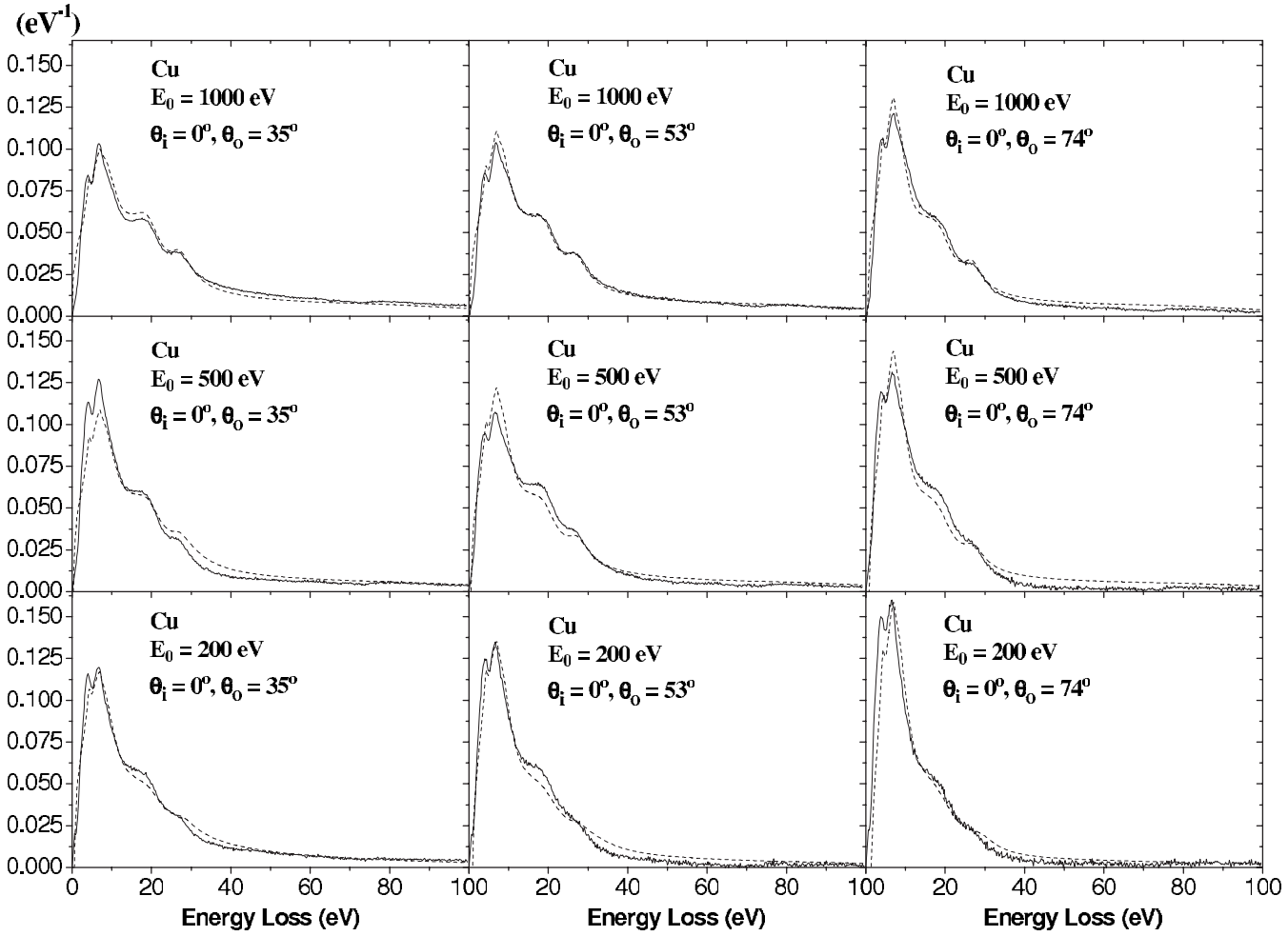

FIG. 7. $\lambda^* K_{\mathrm{exp}}$ (solid line) and $\lambda^* K_{\mathrm{th}}$ (dashed line).

well-established Kramers–Kronig sum rule,[27]

$$\frac{2}{\pi}\int_0^\infty \mathrm{Im}\left\{\frac{1}{\varepsilon(0,\Delta E)}\right\}\frac{d(\Delta E)}{\Delta E} = 1 - \mathrm{Re}\left(\frac{1}{\varepsilon(0,0)}\right). \quad (6)$$

Once the experimental inelastic cross section $K_{\mathrm{exp}}(E_0,\Delta E)$ has been determined, Eq. (4) is used in the calculation of $K_{\mathrm{th}}(E_0,\Delta E)$ as a test function in a trial-and-error procedure, and parameters are modified until the agreement between the theoretical $K_{\mathrm{th}}(E_0,\Delta E)$ and experimental inelastic cross sections $K_{\mathrm{exp}}(E_0,\Delta E)$ is satisfactory.

Analytical expressions have been calculated by Yubero *et al.*[8] for the effective inelastic-scattering cross section $K_{\mathrm{eff}}(E_0,\Delta E,x_0,\theta_i,\theta_o)$ for a *single* REELS electron as a function of their primary energy E_0, the dielectric function of the system $\varepsilon\ (k,\Delta E)$, the maximum depth x_0 reached by the electron before being elastically backscattered, and the incidence θ_i and exit θ_o angles of the electron with respect to the surface normal. However, the cross section determined from an experimental REELS spectrum,[20] by Eq. (1′), has contributions from electrons that have reached different depths in the solid. To compare this cross section with theory, it is necessary to estimate the path-length distribution for those electrons that have undergone a single inelastic-scattering event.

For all elements, small-angle elastic scattering is highly favored, and these events do not significantly affect the trajectory. Furthermore, detailed Monte Carlo calculations show that most of the observed REELS electrons in the energy range of interest have undergone a single large-angle scattering event.[23] Then, for fixed incidence θ_i and exit θ_o angles, the contribution to the measured inelastic-scattering cross section $K_{\mathrm{th}}(E_0,\Delta E,\theta_i,\theta_o)$ is a weighted average over the total path length x of $K_{\mathrm{eff}}(E_0,\Delta E,x_0,\theta_i,\theta_o)$, with the weight function given by $Q(E_0,x,\theta_i,\theta_o)$ as

$$K_{\mathrm{th}}(E_0,\Delta E,\theta_i,\theta_o) = \frac{\int_0^\infty dx Q(E_0,x,\theta_i,\theta_o) K_{\mathrm{eff}}(E_0,\Delta E,x_0,\theta_i,\theta_o)}{\int_0^\infty dx Q(E_0,x,\theta_i,\theta_o)}, \quad (7)$$

where Q is the path-length distribution function for those electrons that have undergone a single inelastic collision. We emphasize again that the theoretical K_{th} in Eq. (7) includes both surface and bulk effects. Thus, we do not calculate

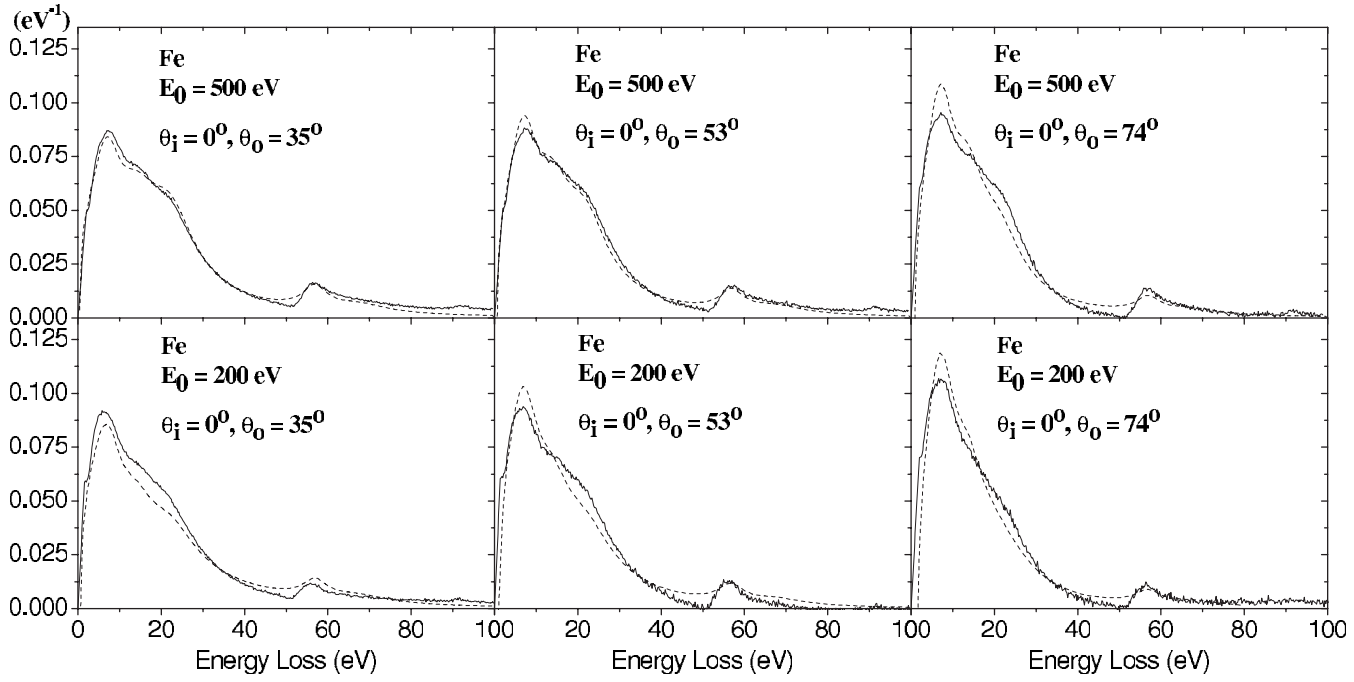

FIG. 8. $\lambda^* K_{exp}$ (solid line) and $\lambda^* K_{th}$ (dashed line).

separate surface and bulk excitations, as was done, e.g., in the models of Chen and co-workers[5,13,14] and Werner.[10,11]

If we assume that the inelastic events are independent, the scattering probability along the path traveled by the electron will be given by a Poisson distribution. Then, the probability that one electron has had only one inelastic scattering is $(x/\lambda_{eff})e^{-x/\lambda_{eff}}$, where λ_{eff} is an "effective" inelastic mean free path for a single REELS electron. It can be calculated by the QUEELS-ε (k, ω)-REELS software[9] as a self-consistent value determined as the inverse of the area of the effective cross section for each trajectory.

We also calculate λ^* by normalizing the two cross sections, i.e.,

$$\lambda^* = \frac{\int (\lambda^* K_{exp}) d(\Delta E)}{\int K_{th} d(\Delta E)}, \tag{8}$$

where integration is done over the energy ranges 2.6–50 eV for Cu, Ag, and Au and 2.6–70 eV for Fe, which contain the main energy-loss structure for these materials.

TABLE II. λ_{TPP} (Å) from Ref. 15 and the calculated λ^* (Å) by Eq. (8) using values in Table I (see text).

	E_0 (eV)	min(λ^*)	max(λ^*)	Ave(λ^*)	λ_{TPP} (Å)
Ag	200	3.68	4.96	3.97	5.29
	500	8.03	10.25	8.92	9.04
	1000	13.73	18.44	16.79	14.75
Au	200	3.79	4.65	4.03	4.62
	500	6.43	8.33	7.21	7.65
	1000	11.91	15.03	13.17	12.31
Cu	200	3.89	4.59	4.27	5.38
	500	7.41	9.51	8.75	9.40
	1000	13.16	17.17	15.16	15.45
Fe	200	3.55	4.05	3.84	5.79
	500	7.08	8.21	7.74	9.99

III. EXPERIMENT

Since the maximum spectral intensity is much lower in the energy-loss range compared to the elastic region, the elastic and inelastic part of the REELS spectra were recorded separately. Thus, to improve the signal to noise level, the inelastic regions of the spectra were recorded in the energy range $E < E_0 - 2$ eV with a higher beam current. The elastic spectrum was measured in a limited energy range around the elastic peak ($E_0 - 9$ eV $< E < E_0 + 2$ eV) with a low primary beam current to make sure that the detector response is linear. The measured elastic and inelastic spectra corresponding to each material at a given geometry and primary electron energy were normalized to their area in the energy interval of $E_0 - 9$ eV to $E_0 - 2$ eV, and a single spectrum that includes the elastic peak and the full energy-loss spectrum was produced.

The REELS spectra of Cu, Ag, Au, and Fe were measured in a ADES 400 photoelectron spectrometer for normal incidence ($\theta_i = 0$) and emission angles θ_o (to the surface normal) from 35° to 74° with a 3° angle step. Primary electron energies of 200, 500, and 1000 eV were used. All spectra were measured using a 20 eV pass energy and a 0.2 eV energy step over a wide energy-loss range (~100 eV). Under these

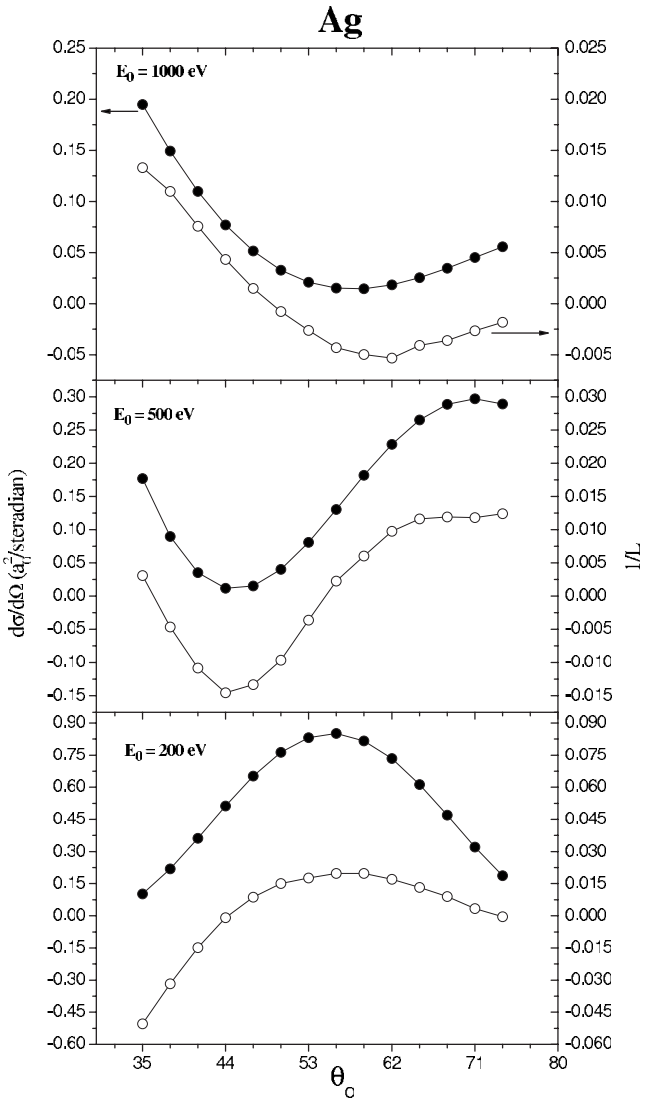

FIG. 9. The determined $1/L$ (Å^{-1}) (open circle) for Ag, using the YT model, and elastic-scattering cross section (solid circle) taken from Ref. 41. a_0 is the Bohr radius.

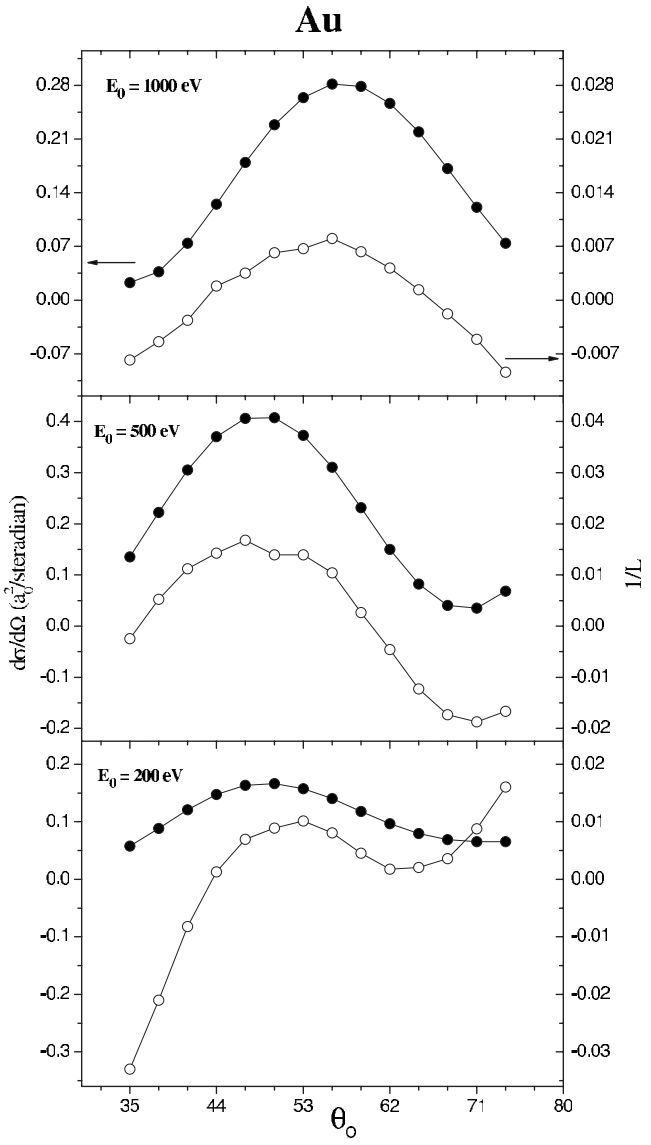

FIG. 10. The determined $1/L$ (Å^{-1}) (open circle) for Au, using the YT model, and elastic-scattering cross section (solid circle) taken from Ref. 41. a_0 is the Bohr radius.

experimental conditions, the full width at half maximum of the elastic peak was ~0.6 eV. The measured spectra were corrected by the analyzer transmission function $T(E) \propto E^{-p}$, where $p=0.64$ for $E_{\text{pass}}=20$ eV.[28]

IV. ANALYSIS, RESULTS, AND DISCUSSION

We used the QUASES-XS-REELS software[29] which applies Eq. (1′) to obtain the experimental $\lambda^* K_{\text{exp}}$ from the REELS spectra.

To determine the ELF of the materials and also to model the theoretical cross section, K_{th}, we used the QUEELS-ε (k, ω)-REELS software,[9] which has been set up on the basis of the formalism mentioned in Sec. II B. From the features observed in the REELS spectra, we assumed a trial ELF for each material. This ELF was modified until the best overall agreement between the theoretical K_{th} and experimental $\lambda^* K_{\text{exp}}$ for all experiments was achieved. The oscillator strengths were renormalized to fulfill the Kramers–Kronig sum rule [Eq. (6)], where $\text{Re}[1/\varepsilon(0,0)]=(n^2-\kappa^2)/(n^2+\kappa^2)^2$. The refractive indices n and the extinction coefficients κ for the studied materials in the long wavelength limit were taken from Ref. 30. For these materials, $\text{Re}[1/\varepsilon(0,0)] \approx 0$, as expected for conductors. Its exact value is therefore not critical. The obtained parameters for the ELFs for these materials are tabulated in Table I and illustrated in Figs. 1–4. For comparison, ELF from Palik[31,32] are also depicted in Figs. 1–4. The agreement with Palik is reasonable for $\hbar\omega < 30$ eV, while it is bad for $\hbar\omega > 30$ eV. The origin of this is unknown. However, note that Palik took the data for Ag, Au, and Fe for the <30 eV and >30 eV energy regions from different publications. Note also that the data[33–37] are ~25–40 years old and may be subject to experimental uncertainties caused, e.g., by surface contamination. Deviations from Palik's data were also reported by Werner,[38,39] who additionally found a gen-

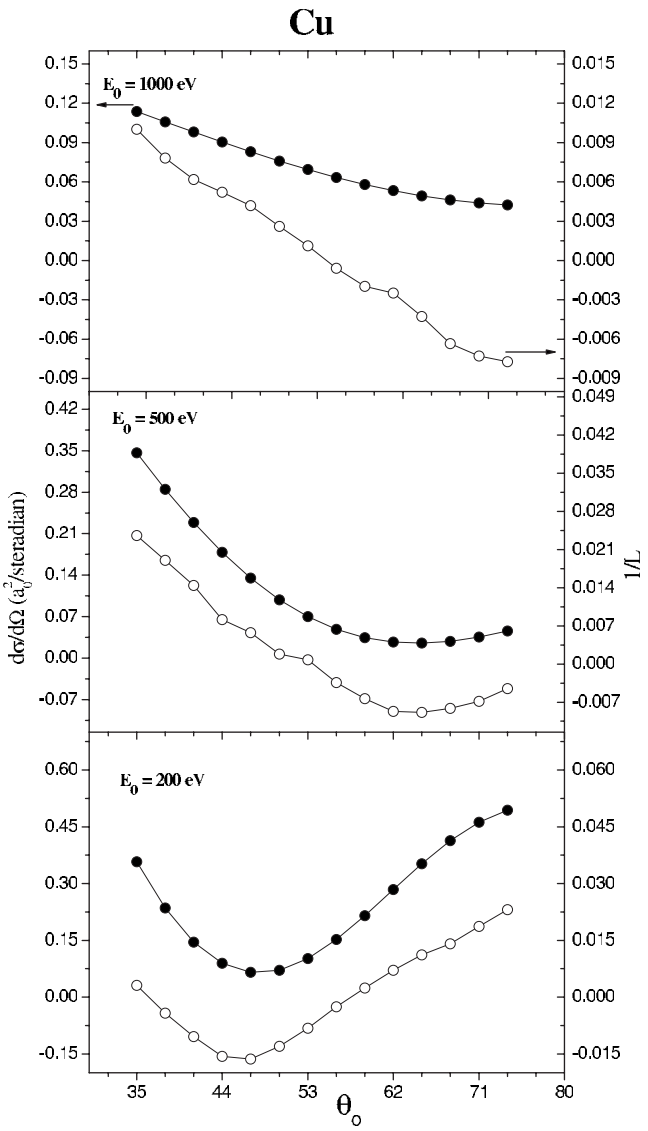

FIG. 11. The determined $1/L$ (Å^{-1}) (open circle) for Cu, using the YT model, and elastic-scattering cross section (solid circle) taken from Ref. 41. a_0 is the Bohr radius.

erally better agreement with calculations based on density functional theory.[38,40]

To see to what extent the shape of K_{th} agrees with the shape of $\lambda^* K_{\text{exp}}$, the normalized theoretical and experimental cross sections are shown in Figs. 5–8 for the studied materials. The normalization factors are tabulated in Table II (see discussion below). Note that in all the calculations, the same ELF was used for each material. The agreement between theory and experiment is quite good for all angles and all energies for each material, and the experimentally observed variation with angle and energy is well described by the theory. One exception is the small peak at ~57 eV for Fe where the theory gives a much wider peak with $\alpha=1$ (corresponding to a free electron dispersion). Using $\alpha=0$ for that oscillator results in a much better agreement between theory and experiment. This peak is mainly due to excitation of the strongly bound Fe $3p$ core electrons, which is the reason why the dispersion is small. A similar effect of $\alpha \approx 0$ has been observed for insulators.[16,24]

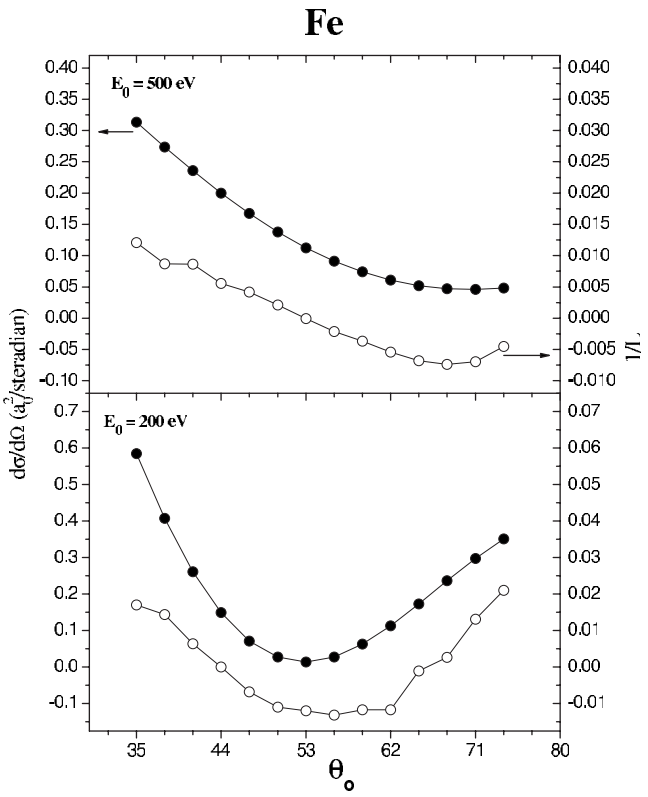

FIG. 12. The determined $1/L$ (Å^{-1}) (open circle) for Fe, using the YT model, and elastic-scattering cross section (solid circle) taken from Ref. 41. a_0 is the Bohr radius.

The fact that the YT theory gives a good agreement with experimental effective cross sections determined by the Tougaard–Chorkendorff algorithm for a very wide range of geometries (35°–74° off normal), and energies 200, 500, and 1000 eV for several materials (Cu, Ag, Au, and Fe) all obtained with the same ε for each material shows that this theory gives a valid and quite accurate description of the dielectric properties. Furthermore, the fact that it is valid for low energies (at least down to 200 eV where $\lambda < 0.5$ nm) proves that it can be used to determine the dielectric properties of nanofilms by an analysis of REELS, and the additional fact that the theory can predict the variation with angle suggests that the method might also be used to determine the dielectric properties of nanostructures.

The obtained values of λ^* are given in Table II for each material at different primary electron energies. The minimum, maximum, and average values of λ^* (averaged over all measured angles) as well as $\lambda_{\text{TPP-2M}}$ (calculated with the QUASES-TPP-2M calculator, which can be freely downloaded from www.quases.com (Ref. 29); this calculator uses the TPP-2M formula by Tanuma *et al.*[15]) are shown in Table II. For each material at a given energy, the obtained value of λ^* depends on the geometry. As can be seen in Table II, the variation of λ^* with geometry for a given material and energy is about 10%–20%. This variation could be due to surface excitations, which could cause λ^* to depend on geometry, or it could be due to the effect of elastic scattering and thereby due to variation in L, which indicates either an increasing or a decreasing path-length distribution (see below).

Note also that although the presented mean values of λ^* are close to $\lambda_{\text{TPP-2M}}$ in most cases, we do not expect to get exactly the same value because $\lambda_{\text{TPP-2M}}$ is for the bulk, on one hand. On the other hand, the expected accuracy of the absolute $\lambda_{\text{TPP-2M}}$ values is $\sim 20\%$.

For the determination of the experimental $\lambda^* K_{\text{exp}}$ by Eq. (1′), it is assumed that the distribution of path lengths R, for $R < 3\lambda$, can be approximated by $e^{-R/L}$. For geometries where the elastic-scattering cross section is low, a large fraction of the detected REELS electrons have undergone multiple scattering events. Therefore, it is expected that L is negative. It should be noted that the Tougaard–Chorkendorff[20] theory is valid also for $L < 0$. L does not have to be positive; and a negative L simply means that the path-length distribution (PLD) increases for small path lengths. The fact that $e^{-R/L}$ approaches infinity for large R is not a problem because only path lengths $<3\lambda$ are relevant for REELS experiments. For geometries where the elastic-scattering cross section is high, most detected electrons have undergone a single scattering event. Therefore, it is expected that L is positive. In order to study if this interpretation is correct, we have calculated L values for each material at a given energy and geometry from Eq. (3) by using the corresponding obtained λ^* and taking λ to be the average values of λ^* (averaged over all measured angles). The resulting $1/L$ values, which indicate either an increasing or decreasing path-length distribution for a given experiment, are shown in Figs. 9–12. The elastic electron scattering cross sections[41] are also shown in Figs. 9–12. As seen, the variation of $1/L$ versus θ_o correlates very well with the elastic-scattering cross section. The values are also seen to be in agreement with the expectations mentioned above. This supports the validity of the assumed simple path-length distribution function.

V. CONCLUSION

From an analysis of extensive REELS experiments, we have studied the validity of the YT theory to determine the dielectric properties of surface nanofilms. The possible limitations due to the assumption of a simple path-length distribution in the method as well as the surface-bulk mixing when the experimental cross section is determined by the Tougaard–Chorkendorff algorithm were studied.

It was found that the YT theory gives a very good agreement with experimental effective cross section for the materials Cu, Ag, and Au at energies 200, 500, and 1000 eV and for Fe at energies 200 and 500 eV for normal electron incidence and emission angles from 35° to 74° with a 3° angle step. It is important to note that the comparison of theory to experiment is done with the same dielectric function ε for all geometries and energies for a given material.

The fact that the theory applies at energies at least down to 200 eV where the inelastic mean free path is ~ 0.5 nm implies that the method can be used to determine the dielectric properties of nanofilms, and the additional fact that the theory can predict the variation with angle suggests that the method might also be used to determine the dielectric properties of nanostructures.

ACKNOWLEDGMENTS

The support by the Institutional Research Plan (No. AV0Z10100521), the Czech Science Foundation (Project No. 202/06/0459), and the Iranian Ministry of Science, Research and Technology (Project No. 42/5/58107—12/8/83) is acknowledged.

[1] R. F. Egerton, *Electron Energy-Loss Spectroscopy in the Electron Microscopy*, 2nd ed. (Plenum, New York, 1996).
[2] G. Chiarello, E. Colavita, M. De Crescenzi, and S. Nannarone, Phys. Rev. B **29**, 4878 (1984).
[3] Y. Ohno, Phys. Rev. B **39**, 8209 (1989).
[4] J. C. Ingram, K. W. Nebesny, and J. E. Pemberton, Appl. Surf. Sci. **44**, 279 (1990).
[5] C. J. Tung, Y. F. Chen, C. M. Kwei, and T. L. Chou, Phys. Rev. B **49**, 16684 (1994).
[6] F. Yubero and S. Tougaard, Surf. Interface Anal. **19**, 269 (1992).
[7] F. Yubero and S. Tougaard, Phys. Rev. B **46**, 2486 (1992).
[8] F. Yubero, J. M. Sanz, B. Ramskov, and S. Tougaard, Phys. Rev. B **53**, 9719 (1996).
[9] S. Tougaard and F. Yubero, Surf. Interface Anal. **36**, 824 (2004); information on the software can be found at www.quases.com
[10] W. S. M. Werner, Surf. Sci. **588**, 26 (2005).
[11] W. S. M. Werner, Phys. Rev. B **74**, 075421 (2006).
[12] W. S. M. Werner, M. R. Went, and M. Vos, Surf. Sci. **601**, L109 (2007).
[13] Y. F. Chen and C. M. Kwei, Surf. Sci. **364**, 131 (1996).
[14] Y. F. Chen, Phys. Rev. B **58**, 8087 (1998).
[15] S. Tanuma, C. J. Powell, and D. R. Penn, Surf. Interface Anal. **21**, 165 (1993).
[16] F. Yubero, J. M. Sanz, J. F. Trigo, E. Elizalde, and S. Tougaard, Surf. Interface Anal. **22**, 124 (1994).
[17] F. Yubero, D. Fujita, B. Ramskov, and S. Tougaard, Phys. Rev. B **53**, 9728 (1996).
[18] H. Jin, S. K. Oh, H. J. Kang, and S. Tougaard, J. Appl. Phys. **100**, 083713 (2006).
[19] H. Jin, S. K. Oh, Y. J. Cho, H. J. Kang, and S. Tougaard, J. Appl. Phys. **102**, 053709 (2007).
[20] S. Tougaard and I. Chorkendorff, Phys. Rev. B **35**, 6570 (1987).
[21] S. Tougaard and J. Kraaer, Phys. Rev. B **43**, 1651 (1991).
[22] P. Prieto, S. Hofmann, E. Elizalde, and J. M. Sanz, Surf. Interface Anal. **36**, 1392 (2004).
[23] N. Pauly, F. Yubero, A. Dubus, and S. Tougaard, Phys. Rev. B (to be published).
[24] F. Yubero, S. Tougaard, E. Elizalde, and J. M. Sanz, Surf. Interface Anal. **20**, 719 (1993).
[25] P. Prieto, F. Yubero, E. Elizalde, and J. M. Sanz, J. Vac. Sci. Technol. A **14**, 3181 (1996).
[26] G. G. Fuentes, E. Elizalde, F. Yubero, and J. M. Sanz, Surf. Interface Anal. **33**, 230 (2002).
[27] J. Daniels, C. V. Festenberg, H. Raether, and K. Zeppenfeld, *Springer Tracts in Modern Physics* Vol. 54, edited by G. Höhler (Springer-Verlag, New York, 1970).

[28] P. Jiricek, Czech. J. Phys. **44**(3), 261 (1994).
[29] www.quases.com
[30] www.luxpop.com
[31] E. D. Palik, *Handbook of Optical Constants of Solids* (Academic, New York, 1985).
[32] E. D. Palik, *Handbook of Optical Constants of Solids* (Academic, New York, 1991).
[33] H. J. Hagemann, W. Gudat, and C. Kunz, J. Opt. Soc. Am. **65**, 742 (1975).
[34] G. Leveque, C. G. Olson, and D. W. Lynch, Phys. Rev. B **27**, 4654 (1983).
[35] L. R. Canfield, G. Hass, and W. R. Hunter, J. Phys. (Paris) **25**, 124 (1964).
[36] T. J. Moravec, J. C. Rife, and D. L. Dexter, Phys. Rev. B **13**, 3297 (1976).
[37] V. P. Shirokovskii, M. M. Kirillova, and N. A. Shilkova, Sov. Phys. JETP **55**, 464 (1982); Zh. Eksp. Teor. Fiz. **82**, 784 (1982).
[38] W. S. M. Werner, Surf. Sci. **600**, L250 (2006).
[39] W. S. M. Werner, Surf. Sci. **601**, 2125 (2007).
[40] W. S. M. Werner, Appl. Phys. Lett. **89**, 213106 (2006).
[41] NIST Electron Elastic-Scattering Cross-Section Database, SRD 64, Version 3.1, standard data program, National Institute of Standards and Technology, Gaithersburg, MD, 2003.